



Can Raman Spectroscopy be Applied for Investigating Graphite Growth in Nodular Cast Irons

Rawen Jday, Olivier Marsan, Jacques Bourdie, Lydia Laffont-Dantras, Fabien Bruneseaux, Jacques Lacaze

► To cite this version:

Rawen Jday, Olivier Marsan, Jacques Bourdie, Lydia Laffont-Dantras, Fabien Bruneseaux, et al.. Can Raman Spectroscopy be Applied for Investigating Graphite Growth in Nodular Cast Irons. Transactions of the Indian Institute of Metals, 2015, 68 (6), pp.1071-1074. 10.1007/s12666-015-0649-y . hal-01472711

HAL Id: hal-01472711

<https://hal.science/hal-01472711>

Submitted on 21 Feb 2017

HAL is a multi-disciplinary open access archive for the deposit and dissemination of scientific research documents, whether they are published or not. The documents may come from teaching and research institutions in France or abroad, or from public or private research centers.

L'archive ouverte pluridisciplinaire **HAL**, est destinée au dépôt et à la diffusion de documents scientifiques de niveau recherche, publiés ou non, émanant des établissements d'enseignement et de recherche français ou étrangers, des laboratoires publics ou privés.



Open Archive TOULOUSE Archive Ouverte (OATAO)

OATAO is an open access repository that collects the work of Toulouse researchers and makes it freely available over the web where possible.

This is an author-deposited version published in : <http://oatao.univ-toulouse.fr/>
Eprints ID : 16701

To link to this article : DOI:10.1007/s12666-015-0649-y
URL : <http://dx.doi.org/10.1007/s12666-015-0649-y>

To cite this version : Jday, Rawen and Marsan, Olivier and Bourdie, Jacques and Laffont-Dantras, Lydia and Bruneseaux, Fabien and Lacaze, Jacques *Can Raman Spectroscopy be Applied for Investigating Graphite Growth in Nodular Cast Irons.* (2015) Transactions of the Indian Institute of Metals, vol. 68 (n° 6). pp.1071-1074. ISSN 0972-2815

Any correspondence concerning this service should be sent to the repository administrator: staff-oatao@listes-diff.inp-toulouse.fr

Can Raman Spectroscopy be Applied for Investigating Graphite Growth in Nodular Cast Irons

Rawen Jday¹ · Olivier Marsan¹ · Jacques Bourdie^{1,2} · Lydia Laffont¹ ·
Fabien Bruneseaux² · Jacques Lacaze¹

Abstract Growth of graphite during solidification and high temperature solid-state transformation has been investigated in samples cut out from a thin wall casting solidified partly in the stable (iron-graphite) and partly in the metastable (iron-cementite) systems. To this end, Raman spectroscopy has been used to characterize graphite nodules in as-cast state and in samples which have been fully graphitized at various temperatures in the austenite field. The results show no significant difference between Raman spectra recorded from these samples, suggesting that graphite grows with the same mechanism during either solidification or high-temperature (so-called first stage) graphitization. Transmission electron microscopy investigation is underway for complementing and checking these results.

Keywords Raman spectroscopy · Graphite · Nodular cast iron

1 Introduction

Raman spectroscopy has been used since long for studying various carbon materials, e.g. graphite precipitates or pyrolytic graphite. It thus seems justified to investigate the possibilities of using Raman spectroscopy for studying graphite precipitates in nodular cast irons formed during solidification or by means of solid-state heat-treatment.

✉ Jacques Lacaze
jacques.lacaze@ensiacet.fr

¹ CIRIMAT, Université de Toulouse, Toulouse, France

² Saint-Gobain Pont-à-Mousson, Pont-À-Mousson, France

Amongst other authors, Reich and Thomsen [1] have reviewed experimental and theoretical features of Raman spectroscopy of graphite. The nomenclature of the bands used by these authors will be followed here. Single-crystal graphite presents three main bands denoted by G, D* and G*. The G band (at about 1583 cm^{-1}) corresponds to the E_{2g} in plane vibrational mode. This should be the only one observed in perfect graphite crystals, together with its very small overtone G* band which appears at a slightly higher frequency than expected (at 3166 cm^{-1}). However, even in perfect single crystals, a strong D* band shows up which is related to double resonance [1]. This D* band is the overtone of the D band (at 1370 cm^{-1}) that appears in disordered graphite [2]. Tuinstra and Koenig [2] related the intensity of the D band to the crystallite size, and it is now accepted that the D band relates to any kind of disorder [1]. Finally, disordering also leads to a shoulder of the G peak, the D' band.

Lespade et al. [3] have systematically investigated carbon deposits graphitized to various states by heat treatment. They found four possible graphitization indexes to characterize disorder: i) position of the G band; ii) width of the G band; iii) ratio I_D/I_G of the intensities of the D (I_D) and G (I_G) bands; iv) width of the D* band. All of these parameters are reported to strongly correlate with d_{002} distance and with magnetic susceptibility. Cuesta et al. [4] investigated a broader range of graphite structures and claimed that the $I_D/(I_D + I_G)$ and the width of the D band should be the preferred disorder parameters. Tsu et al. [5] noted experimentally that the D peak becomes sharper as its strength goes higher, relating this to a narrowing of the density of state which indicates an effect of distortion in the crystal structure.

Tuinstra and Koenig [2] have reported a linear relation between I_D/I_G and the inverse of the size of the graphite crystallites, La: $I_D/I_G = 4.4 \cdot \text{La}^{-1}$ where La is expressed in

nm. Their relation has been used by Nemanich and Solin [6] to evaluate crystallite or domain sizes ranging between 25 Å and 1 µm. Ferrari and Robertson [7] studied an extensive family of disordered and amorphous carbon materials and reported that the La^{-1} type of law applies for La higher than 2 nm. Cançado et al. [8] used the integrated intensities of the D (A_D) and G (A_G) peaks and investigated the effect of the laser wavelength λ_{laser} . They ended up with the relation $A_D/A_G = (2.4 \times 10^{-10}) \lambda_{\text{laser}}^4 (\text{La})^{-1}$, with both λ_{laser} and La expressed in nm. This expression has the same form as the one reported by Tuinstra and Koenig, but the constant here is three times larger as against those by other authors [8].

Though Raman spectroscopy appears very well suited for studying graphite in cast iron which is known to present various kinds of defects, very little studies have been found in the literature. Hirlmann et al. [9] analyzed samples with lamellar graphite and reported domains of 4.5–6.5 nm by using the relation proposed by Tuinstra and Koenig. Cooper et al. [10] compared lamellar and spheroidal graphite using a laser beam focused to a spot of size 2 µm. By deconvolution of the D^* band into two peaks, they observed that the intensity of one of them was constant from which they concluded that the graphite precipitates were stress free. Estandia et al. [11] suggested Raman spectroscopy for evaluating residual stress in cast iron, i.e. using graphite precipitates as stress sensors. On tensile test specimens ruptured at ca. 240 MPa, they observed a 4 cm⁻¹ decrease of the G band shift. Using data from literature [12], the authors concluded on a residual tensile stress of 830 MPa. Finally, Amini et al. [13] used I_D/I_G for estimating the number of layers in graphene obtained from the surface of carbon saturated Ni-C melts. The present investigation makes use of Raman spectroscopy to look for any differences in graphite nodules formed during solidification or by high-temperature solid-state treatment of cast iron.

2 Experimental Details

A piece of mottled cast iron was taken out from a thin wall casting and cut in four samples. The first sample was left as-cast while the others were fully graphitized by heat-treating at 850 °C (60 min), 950 °C (20 min) and 1050 °C (5 min) respectively, and then cooled in air. The samples were then finally cut to give a transverse section (perpendicular to their surface). The four sections were prepared for observation by standard metallographic technique. The diameter of the largest nodule was found to vary from 8.5 µm in the as-cast sample to 11 µm in the one heat-treated at 850 °C.

Raman spectroscopy was carried out using a Labram HR800 micro-Raman spectrometer equipped with a green

laser (wave length λ of 532 nm). The laser power was 13 mW and the light was polarized vertically by construction. Two density filters were used to protect graphite from beam damage. The Raman spectra were collected in the backscattering configuration using a confocal microscope with a 100× objective. The spectral resolution was 2.2 cm⁻¹ (in relation with the 600 lines/mm grating used for recording the spectra), and the focused laser beam had a lateral resolution of 0.7 µm and a resolution of 2.6 µm in the direction of the laser beam. Measurement points were recorded along lines with a step of 0.5 µm, and maps could be generated by recording successive line scans 0.5 µm apart. Every spectrum was recorded in the range of 1000–1900 cm⁻¹ during 60 s.

Figure 1 shows a typical example of Raman spectrum obtained in this study. It exhibits two main peaks, corresponding to the D (1349.4 cm⁻¹) and G (1580.8 cm⁻¹) bands, as well as the D' band (1620.3 cm⁻¹) which appears as a shoulder of the G band. Using LabSpec5 software package, the experimental spectra were fitted with Gaussian–Lorentzian mixed curves which are shown as thin lines in the graph. This fitting allowed subtracting the noise, and the intensity of the D and G peaks could be estimated either by their peak values (I_D and I_G) or by their integrated area (A_D and A_G).

3 Results and Discussion

Figure 2 shows the mapping of G and D band intensities for a graphite nodule of the sample treated at 950 °C. In both maps, the presence of sectors emanating from the nodule center and expanding towards its periphery is easily observed. Such sectors are very much similar to those seen while observing spheroids with polarized optical light and they appear here because of the polarized laser beam. It is well known that these sectors are associated with the fact that the graphite *c* direction is radially orientated, and

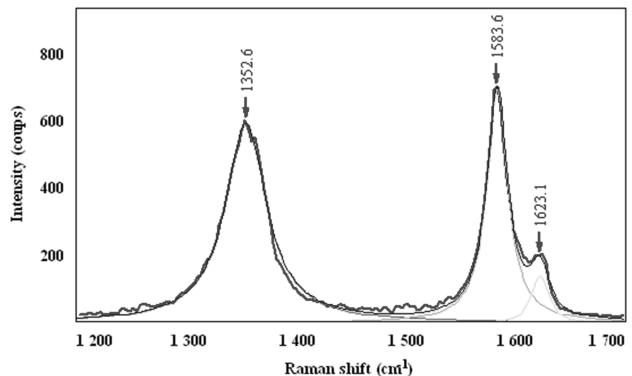


Fig. 1 Example of Raman shift spectrum and of its fitting with Gaussian–Lorentzian functions

marked difference in color between two areas reflects a large difference in crystal orientation.

In all nodules observed, a central zone with a different contrast can be seen which is related with the graphite nucleus. Optical observation shows these zones having a size of 1 to 1.5 μm . Because of the lateral resolution of the Raman spectrometer used in this study, results from the central area with a size of about 2.5 μm in diameter should be disregarded.

Figure 3a shows the I_D/I_G map for the same nodule as in Fig. 2. Excluding the very center of the nodule, the change in the I_D/I_G ratio is limited between 0.8 and 1.2. Figure 3b compares the I_D/I_G and A_D/A_G ratios along the horizontal diameter of the nodule section. It is observed that the curves exhibit similar variation along this diameter, and it has been verified that this applies for any diametrical scan. If the central area is excluded, i.e. by not considering the greyed area in the graph, it is seen that I_D/I_G and A_D/A_G values are quite constant at about 0.95 ± 0.2 and 1.4 ± 0.2 respectively. The relation evaluated by Tuinstra and Koenig [2] give crystallite size of about 4.6 nm in agreement with the report by Hirlmann et al. [9]. The use of the relation by Cançado et al. [8] gives 13.7 nm. Both values

appear much smaller than the thickness of the growth blocks reported in the literature for graphite in cast iron, namely 50–500 nm (see for example Theuwissen et al. [14]). This necessitates further investigation using transmission electron microscopy (TEM) or other means.

Other parameters reported in the literature for characterizing disorder were explored. The full widths at half maximum of the D and G bands, denoted by FWHM or Γ in literature, show nearly constant values over all the section of the graphite nodule, including the center, i.e. the area associated to the nucleus. The positions of the D and G peaks show little variation. It thus appears that these quantities can not be used for characterizing disorder in graphite nodules in cast irons.

For every sample, Raman scans along the horizontal diameter of three nodules were recorded, selecting the largest nodules seen in each metallographic section. Figure 4a compares the I_D/I_G ratio for the three nodules observed in the as-cast sample and the one heat-treated at 850 °C, and Fig. 4b for samples heat-treated at 950 and 1050 °C. For each record, the origin of the abscissa has

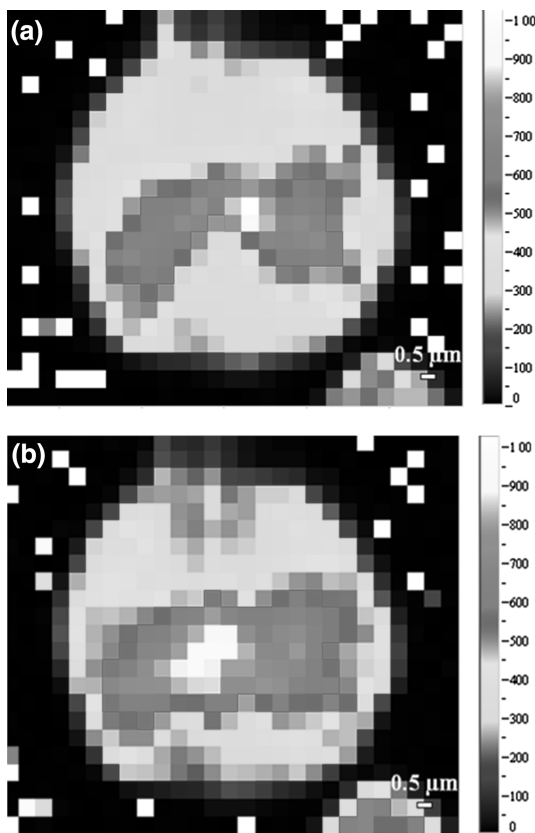


Fig. 2 Example of Raman mapping of the intensities of the **a** D and **b** G bands. The color scale indicates the intensities, it is the same for both maps

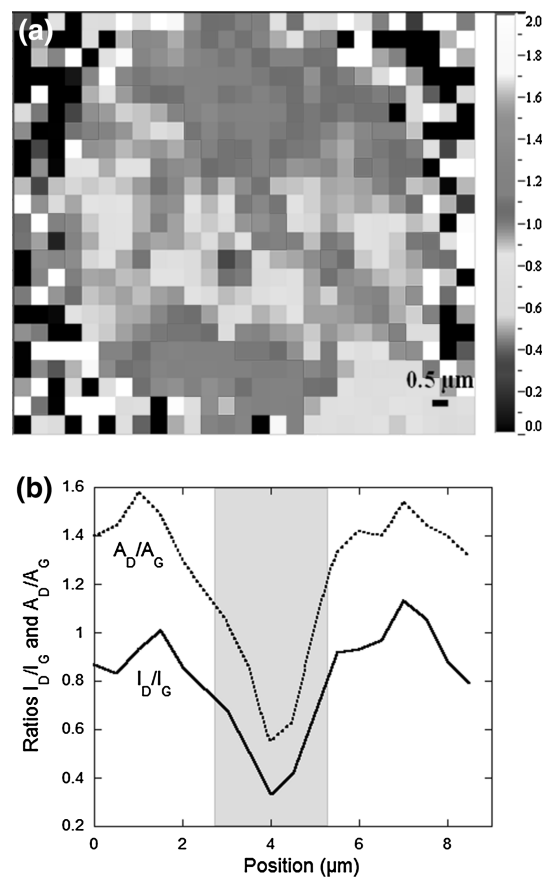


Fig. 3 **(a)** column to the left) I_D/I_G mapping and **(b)**, column to the right) evolution of I_D/I_G and A_D/A_G along the horizontal diameter of the same graphite nodule as in Fig. 2. The color scale along the map indicates the values of the ratio

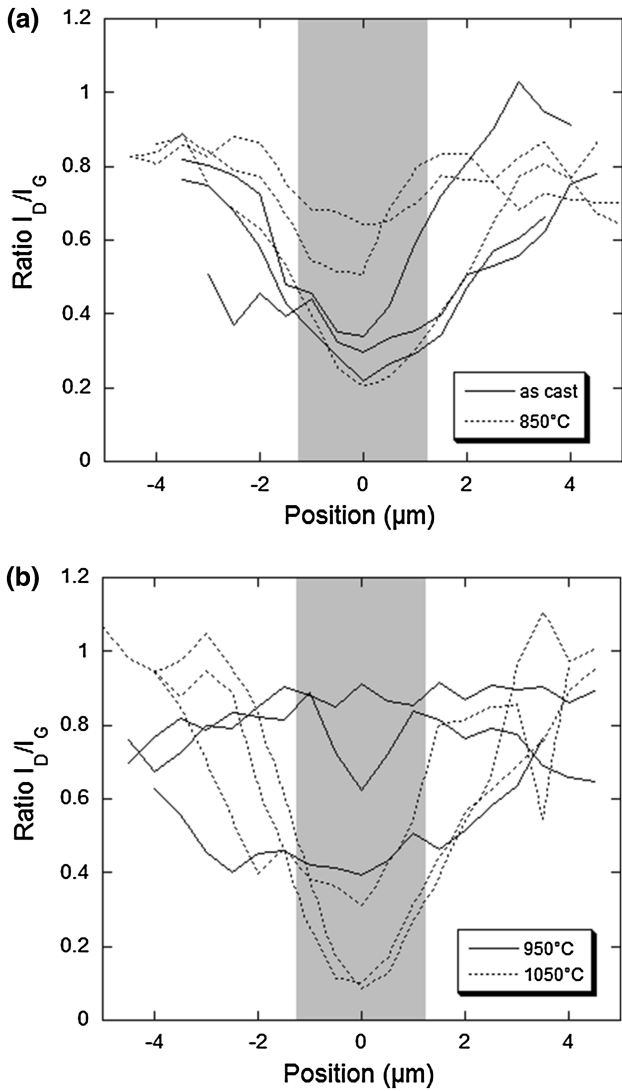


Fig. 4 Evolution of I_D/I_G along the horizontal diameter for the three nodules **a** in the as-cast sample (solid lines) and the sample heat-treated at $850\text{ }^\circ\text{C}$ (dotted lines) and **b** in the samples heat-treated at $950\text{ }^\circ\text{C}$ (solid lines) and $1050\text{ }^\circ\text{C}$ (dotted lines)

been positioned at the location of the minimum of the I_D/I_G ratio. In a few cases, the I_D/I_G ratio appears somehow constant but in most cases it increases with the distance from the nodule center, suggesting a slight increase in graphite disorder during its growth as well as of the crystallite size. Such an increase is unexpected and should be investigated by other means, e.g. TEM.

4 Conclusion

The Raman results reported in this study show values of I_D/I_G which are very similar for all samples, with a slight increase with the distance from the nodule centers. This increase seems astonishing as it would mean an increase in graphite defects during nodule growth. It appears anyway that crystalline defects in graphite grown during solidification or during solid-state heat-treatments are probably similar. This suggests that the graphite growth mechanism could be the same when nodules precipitate during solidification or by cementite decomposition during heat-treatment in the austenitic field. Transmission electron microscopy studies are underway for complementing and checking these results.

References

1. Reich S, and Thomsen C, *Phil Trans R Soc Lond A* **364** (2004) 2271.
2. Tuinstra F, and Koenig J L, *J Chem Phys* **53** (1970) 1126.
3. Lespade P, Marchand A, Couzi M, and Cruege F, *Carbon* **22** (1984) 375.
4. Cuesta A, Dhamelincourt P, Laureyns J, Martinez-Alonso A, and Tascon J M D, *Carbon* **32** (1994) 1523.
5. Tsu R, Gonzalez J H, and Hernandez I C, *Solid State Commun* **27** (1978) 507.
6. Nemanich R J, and Solin S A, *Phys Rev B* **20** (1979) 392.
7. Ferrari A C, and Robertson J, *Phys Rev B* **61** (2000) 14095.
8. Cançado L G, Takai K, Enoki T, Kim Y A, Mizusaki H, Jorio A, Coelho L N, Magalhães-Panagio R, and Pimenta M A, *Appl Phys Lett* **88** (2006) 163106.
9. Hirlmann C, Jouanne M, and Forrières C, *J Raman Spectrosc* **23** (1992) 315.
10. Cooper C A, Elliott R, and Young R, *J Mater Sci* **38** (2003) 795.
11. Estandia B, Rodriguez L, Alvarez J A, Ferreiro D, Hernandez D, and Gonzalez J, *Raman spectroscopy of flake graphite as a tool to detect stress-strain states in cast iron*, World foundry congress (2014). Curran Associates, Inc., NY, ISBN: 978-1-63439-804-6, p 679.
12. Robinson I M, Zakikhani M, Day R J, Young R J, and Gallois C, *J Mater Sci Lett* **6** (1987) 1212.
13. Amini S, Kalaantari H, Garay J, Balandin A A, and Abbaschian R, *J Mater Sci* **46** (2011) 6255.
14. Theuwissen K, Lafont M-C, Laffont L, Viguier B, and Lacaze J, *Trans Indian Inst Met* **65** (2012) 627.